A Temperature Control Technique for Nonequilibrium Molecular Simulation

A temperature control technique for nonequilibrium molecular simulation

Ben Leimkuhler, Frédéric Legoll, and Emad Noorizadeh

Citation: The Journal of Chemical Physics **128**, 074105 (2008); doi: 10.1063/1.2829869
View online: http://dx.doi.org/10.1063/1.2829869
View Table of Contents: http://scitation.aip.org/content/aip/journal/jcp/128/7?ver=pdfcov
Published by the AIP Publishing

A temperature control technique for nonequilibrium molecular simulation

Ben Leimkuhler,[1,a)] Frédéric Legoll,[2,3] and Emad Noorizadeh[1]
[1]*The Maxwell Institute and School of Mathematics, University of Edinburgh, Edinburgh EH9 3JZ, United Kingdom*
[2]*Université Paris-Est, Institut Navier, LAMI, Ecole des Ponts, 77455 Marne-La-Vallée cedex 2, France*
[3]*INRIA Rocquencourt, MICMAC Team-Project, 78153 Le Chesnay cedex, France*

(Received 15 May 2007; accepted 7 December 2007; published online 19 February 2008)

We describe a dynamical approach to thermal regulation in molecular dynamics. Temperature is moderated by a control law and an additional variable, as in Nosé dynamics, but whose influence on the system decreases as the system approaches equilibrium. This device enables approximation of microcanonical averages and autocorrelation functions consistent with a given target temperature. Moreover, we demonstrate that the suggested technique is effective for the control of heat dissipation in a nonequilibrium setting, first by showing that the temperature control correctly regulates heat introduced by a rapid change to the system, and then by studying the slow relaxation of vibrational degrees of freedom (e.g., due to bonded atoms) in a solvent bath. © *2008 American Institute of Physics*. [DOI: 10.1063/1.2829869]

I. INTRODUCTION

When properly used, molecular dynamics (MD) is a powerful technique for resolution of detailed properties of materials. Combined with coarse graining, on the one hand, or quantum mechanics, on the other, MD integration is a crucial component of multiscale or multiphysics simulations, even including a transient (nonequilibrium) phase. In most current simulations, a thermal control mechanism is used to match the temperature of simulation to a laboratory environment. Given a molecular system of N massive particles, the popular Nosé–Hoover dynamics method[1,2] replaces Newtonian dynamics by an extended system of the form

$$\dot{\mathbf{q}}_i = m_i^{-1}\mathbf{p}_i, \tag{1}$$

$$\dot{\mathbf{p}}_i = \mathbf{F}_i - \xi\mathbf{p}_i, \quad i = 1,2,\ldots,N, \tag{2}$$

$$Q\dot{\xi} = \sum_{i=1}^{N} m_i^{-1}p_i^2 - gk_BT, \tag{3}$$

where m_i, $\mathbf{q}_i$, and $\mathbf{p}_i$ are the mass, position vector, and momentum vector, respectively, of the ith atom, $i=1,\ldots,N$, $p_i = \|\mathbf{p}_i\|$, g is the number of degrees of freedom ($3N-d$, where d is the number of conserved quantities), k_B is the Boltzmann constant, and T is temperature. ξ is a variable that regulates the average temperature, and Q is an (artificial) thermostat coefficient that influences the coupling of the thermostat to the system.

The trajectories of this system can be shown to facilitate (exact) canonical sampling under an ergodicity assumption. Nosé–Hoover dynamics (NHD) can thus be viewed as a closed, truncated approximation to a macroscopic system that allows direct recovery of canonical thermodynamic averages from sampling trajectories. Under standard assumptions, microcanonical and canonical ensembles agree in the thermodynamic limit. In many applications, the correction of sampling by Nosé dynamics and other schemes is less important than obtaining the correct temperature, i.e., that $(1/t)\int_0^t \sum_{i=1}^N m_i^{-1}p_i^2(s)ds \to gk_BT$. On the other hand, in Eqs. (1)–(3), convergence of the average temperature *does not* imply $\xi(t)\to 0$; thus, NHD introduces a persistent artificial perturbation of the Newtonian dynamics, which is sometimes severe.[3–6] For example, the thermostat may inhibit large local fluctuations of temperature, which are important in stimulating a transition. In many cases, it would be more appropriate to use Newtonian dynamics at an energy consistent with the desired target temperature.

The idea considered here is to replace Eq. (3) by an alternative differential equation,

$$\frac{d}{dt}\xi = a(t)\left(\sum_{i=1}^{N} m_i^{-1}p_i^2 - gk_BT\right) - b(t)\xi, \tag{4}$$

where the coefficient functions a and $b>0$ are (for the moment) arbitrary bounded functions. The purpose of this equation is to (i) control the temperature of the system while (ii) reducing the influence of the artificial device on the system dynamics once equilibrium is achieved.

Traditionally, the concept of temperature—and the idea of a thermostat—is meaningful for systems in or near thermal equilibrium. In the nonequilibrium setting, we share the perspective of Ruelle[7] "To keep a finite system outside of equilibrium we subject it to non-Hamiltonian forces…. This means that the system will heat up. Indeed, this is what is observed experimentally: Dissipative systems produce heat. An experimentalist will eliminate excess heat by use of a thermostat, and if we want to study nonequilibrium steady states we have to introduce the mathematical equivalent of a thermostat." Thus, we interpret a thermostat in the nonequilibrium context as a practical device: A (mild as possible) perturbation of dynamics that removes excess heat induced by nonequilibrium forces.

In the following sections, we describe the motivation for Eq. (4), propose specific choices for the functions $a(t)$ and $b(t)$ that appear in this equation, and discuss numerical ex-

a)Electronic mail: B.leimkuhler@ed.ac.uk.

periments, which include a comparison with standard (equilibrium) thermostats such as Nosé dynamics and Langevin dynamics.

II. DYNAMICAL THERMOSTATS

Here, we briefly review the Nosé–Hoover method for thermostatting molecular dynamics. Consider a Hamiltonian system with energy function

$$H = \sum_{i=1}^{N} \frac{p_i^2}{2m_i} + U(\{\mathbf{q}_i\}).$$

Nosé dynamics allows thermal regulation via a simple dynamical device based on substituting for the original constant energy model an extended Hamiltonian of the form

$$H_N = H(\{\mathbf{q}_i\},\{\tilde{\mathbf{p}}_i/s\}) + \frac{p_s^2}{2Q} + gk_BT \ln s,$$

where T is the target temperature and Q is a positive parameter that effects the strength of the coupling of physical variables to the bath. The momenta $\tilde{\mathbf{p}}_i$ appearing in H_N should be viewed as canonical to the $\mathbf{q}_i$, whereas the physical momenta $\mathbf{p}_i$ are related to the $\tilde{\mathbf{p}}_i$ by the change of variables,

$$\mathbf{p}_i = \frac{\tilde{\mathbf{p}}_i}{s}.$$

Under an ergodicity assumption, it can be shown that the microcanonical (constant energy) averages for the extended system reduce to canonical phase space averages for the physical system.[1] Rescaling the kinetic energy by a certain factor engenders a transformation of time. The Nosé–Hoover method[2] reverses this time transformation while also reintroducing the physical momenta. With the substitutions $\xi = p_s/Q$, the equations of motion can be written as in Eqs. (1)–(3). These equations are time reversible, but no longer Hamiltonian, due to the form of the time transformation used in their derivation. The automatic determination of optimal Q is, particularly for biomolecules, a challenging problem,[8] but for many common systems such as a Lennard-Jones liquid, canonical sampling is obtained for a wide range of values.

A variety of alternative methods for thermostatting have been proposed based on the idea of augmented dynamics (recent examples and discussion[8,9]). A quite different class of methods is obtained by incorporating stochastic noise (Langevin dynamics[10,11]); we touch on this alternative in Sec. VI.

III. TEMPERATURE-REGULATED DYNAMICS

Instead of a differential temperature control law as in Eq. (3), consider the following algebraic formula to define ξ:

$$\mu\xi = \frac{1}{t}\int_0^t g^{-1}K(s)ds - k_BT, \tag{5}$$

where $K = \Sigma_{i=1}^{N} m_i^{-1} p_i^2$ and μ is a positive parameter. If we assume the cumulative average kinetic energy per degree of freedom were to converge to k_BT with time, then ξ would tend to zero so that the perturbation of constant energy dynamics would be expected to diminish with time. Effective numerical methods for Eqs. (1), (2), and (5) are cumbersome to design and analyze since the equations are in the form of a delay-differential system. We therefore differentiate Eq. (5) with respect to time to obtain

$$\mu\frac{d}{dt}\xi = \frac{1}{t}g^{-1}K - \frac{1}{t^2}\int_0^t g^{-1}K(s)ds$$

$$= \frac{1}{t}(g^{-1}K - k_BT) - \frac{1}{t}\mu\xi, \tag{6}$$

which we recognize to be in form (4) with $a(t) = (g\mu t)^{-1}$ and $b(t) = t^{-1}$. If the term proportional to ξ were absent from Eq. (6), the equation would look similar to the usual Nosé–Hoover formula, but with a gt^{-1} scaling. The t^{-1} term thus acts as a coefficient of damping, which becomes weaker with time, even as the effect of the thermostat is similarly reduced. As described, however, the method has an obvious flaw: Since the control is effectively scaled by $1/t$, the control will be less responsive to a change in state occurring later in the simulation. In nonequilibrium modeling, it is necessary to consider the potential need for reequilibration during simulation.

The idea this suggests is to introduce a time-localized weight function in the computation of the average temperature,

$$\mu\xi = \frac{1}{\hat{\phi}(t)}\int_0^t \phi(t-s)g^{-1}K(s)ds - k_BT, \tag{7}$$

where $\phi(t)$ is the prescribed weight function, and $\hat{\phi}(t)$ its integral on $[0,t]$. Note that Eq. (5) can be recovered as a special case of Eq. (7), with the choice $\phi(t) \equiv 1$. Equations (1), (2), and (7) are again a delay-differential equation system. We now reformulate them as an ordinary differential equation system for the purposes of an efficient numerical treatment.

Introduce a new variable $\Phi = \int_0^t \phi(t-s)g^{-1}K(s)ds$, and set $\mu\xi = [\Phi/\hat{\phi}(t)] - k_BT$. Then, if $\phi(t) = \exp(-t/\tau)$, we have $(d/dt)\Phi = \phi(0)g^{-1}K(t) + \int_0^t \phi'(t-s)g^{-1}K(s)ds = g^{-1}K(t) - \tau^{-1}\Phi$. We thus arrive at an elegant closed differential equation for the controlled system [temperature-regulated dynamics (TRD)] consisting of Eqs. (1) and (2), with ξ determined from

$$\frac{d}{dt}\Phi = g^{-1}K(t) - \tau^{-1}\Phi, \quad \mu\xi = \hat{\phi}^{-1}\Phi - k_BT, \tag{8}$$

where $\hat{\phi}(t) = \tau[1 - \exp(-t/\tau)]$. In the limit $\tau \to +\infty$, we see that $\phi(t)$ becomes constant and equal to 1, and the exponential relaxation system formally becomes the average temperature control system [Eqs. (1), (2), and (6)] that we considered previously. It should be reiterated that the method based on Eqs. (1), (2), and (8) has no defined thermodynamic ensemble. In the sequel, we demonstrate by numerical experiments that it performs in a way that is similar to a microcanonical formulation, when near thermodynamic equilibrium, while maintaining the ability to drive the system temperature during out-of-equilibrium excursions.

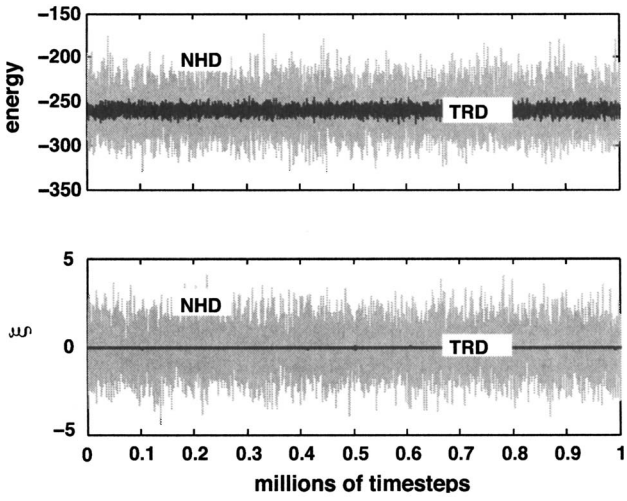

FIG. 1. Comparison of total energy conservation (upper panel) and long term stability of ξ (lower panel) for the TRD method (dark) and Nosé–Hoover (light).

In our experiments, we obtained good results by use of the following discretization scheme:

$$\mathbf{q}_i^{n+1} = \mathbf{q}_i^n + \Delta t m_i^{-1} \mathbf{p}_i^{n+1/2},$$

$$\mathbf{p}_i^{n+1/2} = \mathbf{p}_i^n + \frac{\Delta t}{2}\mathbf{F}_i^n - \frac{\Delta t}{2}\xi^n \mathbf{p}_i^{n+1/2},$$

$$\Phi^{n+1} = \Phi^n + \Delta t g^{-1} K^{n+1/2} - \frac{\Delta t}{2\tau}(\Phi^n + \Phi^{n+1}),$$

$$\mu\xi^{n+1} = \frac{\Phi^{n+1}}{\hat{\phi}(t_{n+1})} - k_B T,$$

$$\mathbf{p}_i^{n+1} = \mathbf{p}_i^{n+1/2} + \frac{\Delta t}{2}\mathbf{F}_i^{n+1} - \frac{\Delta t}{2}\xi^{n+1}\mathbf{p}_i^{n+1/2}.$$

The TRD dynamics are not Hamiltonian or time reversible and have no apparent conserved quantities; thus, it does not make sense to talk about the preservation of these properties under discretization. Nonetheless, we expect that in simulation ξ will become small in the long term (see following sections), and it is useful to observe that the above discretization reduces in the limit $\xi \to 0$ to the symplectic-reversible Verlet method for the constant energy model. As a simple illustration of the method, we performed a simulation of a dense liquid MD model consisting of 108 atoms moving in a Lennard-Jones potential with periodic boundary conditions. Parameters were, in reduced units (i.e., $\sigma_{\mathrm{LJ}}=1.0$, $\epsilon_{\mathrm{LJ}}=1.0$), $T=1.31$, and initial density $\rho=0.9184$. We took $\tau=1$ and $\mu=1$ in our simulations (regarding these as arbitrary parameters that would need to be selected by experimentation for realistic systems). 1×10^6 time steps of size $\Delta t=0.01$ were taken. As we see in Fig. 1, ξ remains small and, judging from the lack of drift in the total energy, the method appears to be quite stable.

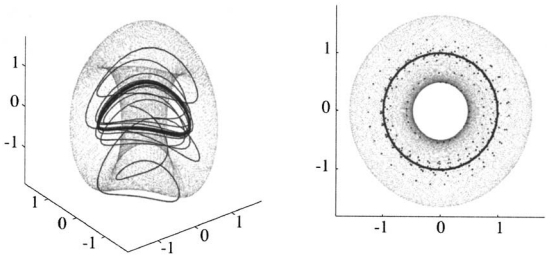

FIG. 2. Collapse of TRD dynamics trajectory (dark) to a lower-dimensional submanifold for a harmonic oscillator; (q,p,ξ) space (left), with projection onto the qp-plane (right). The corresponding NHD trajectory is shown in light gray.

IV. LONG TIME BEHAVIOR

It is possible to perform a partial analysis of the behavior of TRD dynamics in the long time limit. In order to study the long time behavior, we compute the divergence of the TRD vector field: $\kappa=-g\xi-1/\tau$. From its definition, it is apparent that Φ is a positive function, and thus $\xi(t)\geqq -k_B T\mu^{-1}$; hence, it follows that

$$\kappa \leqq k_B T g \mu^{-1} - 1/\tau.$$

Thus, one can choose μ such that $\kappa\leqq-\kappa_c<0$, in which case the phase space volume is contracting: For any set of initial conditions occupying a positive volume, the volume v_t occupied by the corresponding set after some time t goes to 0 as t goes to infinity. In our simulation (see Fig. 1), we verify that ξ remains small ($|\xi(t)|\leqslant 0.05$) and that the trajectory stays on (or close to) a constant energy surface. In Fig. 2, we illustrate a trajectory of the TRD extension for a harmonic oscillator compared with a corresponding Nosé–Hoover trajectory. The Nosé–Hoover trajectory (light) apparently covers the surface of a torus in the (three-dimensional) phase space, and its projection onto the qp-plane fills an annulus.[12] The TRD trajectory (dark) converges to the neighborhood of a constant energy trajectory, in this case a circle, having the desired average kinetic energy.

V. EQUILIBRATION OF A NONADIABATIC PERTURBATION

We now return to the Lennard-Jones model, simulated with the following nonadiabatic perturbation: A rapid increase in the Lennard-Jones radius. In our simulation, we start with the previously described 108 atom model, with the system initially relaxed at temperature $T=1.31$; between time $t=20$ and $t=21$, the parameter σ is increased from $\sigma=1.0$ to $\sigma=1.05$ by successive rescaling at each time step, during which time the box volume is held constant, effectively increasing the system pressure. When microcanonical dynamics is used, the result is as shown in Fig. 3, where we plot the instantaneous average kinetic energy $g^{-1}K(t)$ and the cumulative average kinetic energy $(1/t)\int_0^t g^{-1}K(s)ds$. When the perturbation is applied, there is a rapid drift in temperature, demonstrating that a control mechanism is needed to restore the system temperature during and after the onset of the kick.

We expect the thermostatted scheme to maintain the system at the desired target temperature during the kick. As we see in the upper panel of Fig. 4, Nosé–Hoover (here used

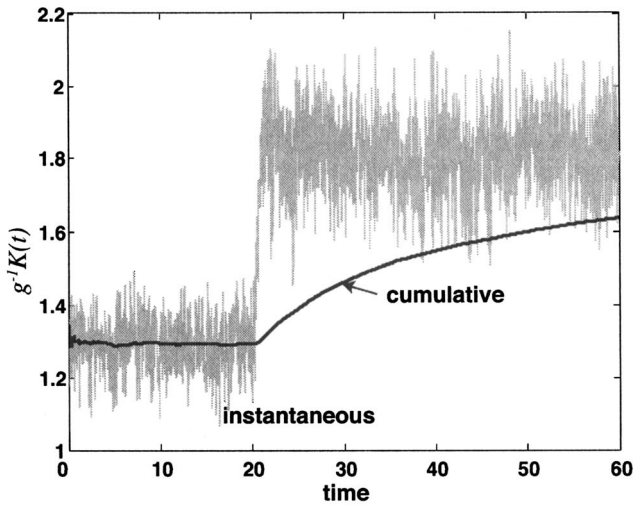

FIG. 3. Recorded kinetic energy per particle $g^{-1}K(t)$ through nonadiabatic perturbation for a microcanonical simulation. The cumulative average kinetic energy [time average of $g^{-1}K(t)$] is shown in bold.

with a target temperature of $T=1.31$ and thermostat parameter $\mu=1$) is able to achieve this. In fact, there is no evidence in the temperature profile that any disturbance was introduced. This also means that in those situations where kinetic fluctuation is the driver for a nonequilibrium process, Nosé–Hoover may unfavorably restrict the extent of those fluctuations.

The TRD scheme also performs the thermalization task, although in a different way (Fig. 4, lower panel). At the onset of the kick, the system is allowed to exhibit a momentary initial rise in temperature. After this initial rise, the system relaxes back to thermal equilibrium at the target temperature. Figure 5 compares the total energy evolution for the three methods. TRD and NHD find the same temperature-regulated value following the perturbation. We also observe in Fig. 5 that the energy fluctuations are smaller with TRD than with NHD. This signifies that the TRD method is close to microcanonical dynamics (while controlling the temperature), whereas NHD is a canonical sampling method. Finally,

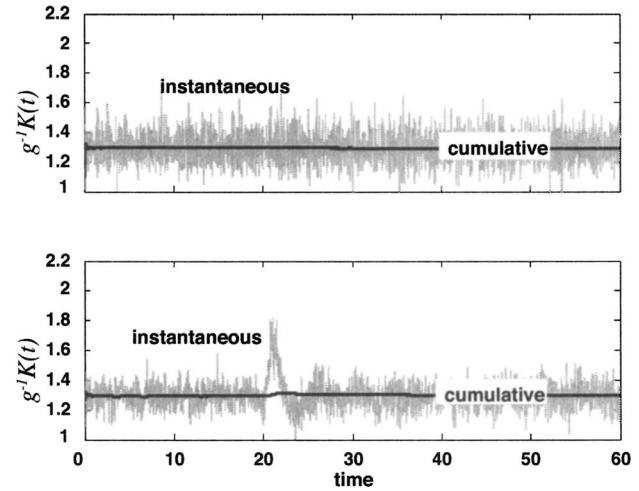

FIG. 4. $g^{-1}K(t)$ through nonadiabatic perturbation for Nosé–Hoover simulation (upper panel) and TRD (lower panel). Cumulative average kinetic energies are shown in bold.

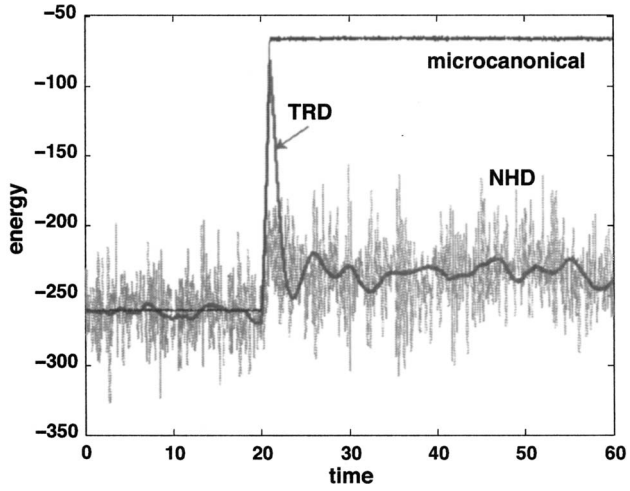

FIG. 5. Comparison of total energy fluctuation for NHD, TRD, and *NVE* simulations.

Fig. 6 shows the comparative evolution of ξ for each of TRD and NHD, demonstrating that the temperature control is always strongly active in NHD, whereas TRD represents a much smaller perturbation and only shows a slight rise to cope with the nonadiabatic change between $t=20$ and $t=21$. These qualitative observations were similar for many choices of the TRD parameter ($0.001<\tau<10$), although the choice of τ does lead to differences in the sensitivity to change in the solution and/or the observed energetic fluctuations.

VI. VIBRATIONAL DIFFUSION

We next study the vibrational diffusion observed in a model consisting of a bonded atom pair in a liquid bath. In the previously described system of 108 atoms of unit mass interacting pairwise with a Lennard-Jones potential, we incorporate a stiff harmonic spring with rest length equal to the Lennard-Jones (LJ) equilibrium separation. The stiffness coefficient was chosen so that the frequency of the resulting vibration was about three times the fastest natural mode of the solvent. The entire system was equilibrated at $k_BT=1.3$, and then the velocity autocorrelation function associated

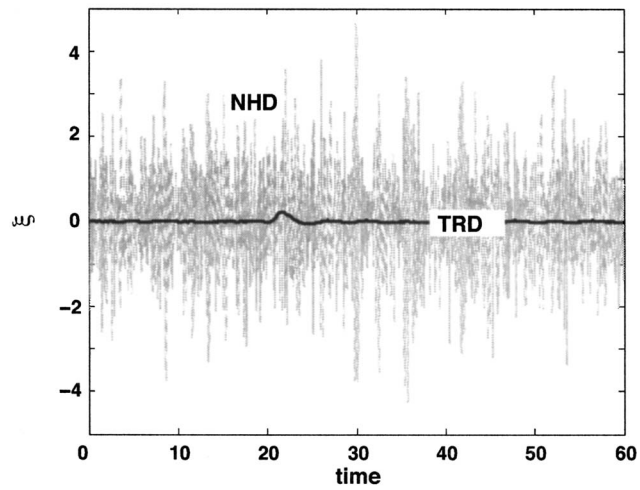

FIG. 6. Variation of ξ using NHD (light) and TRD (bold).

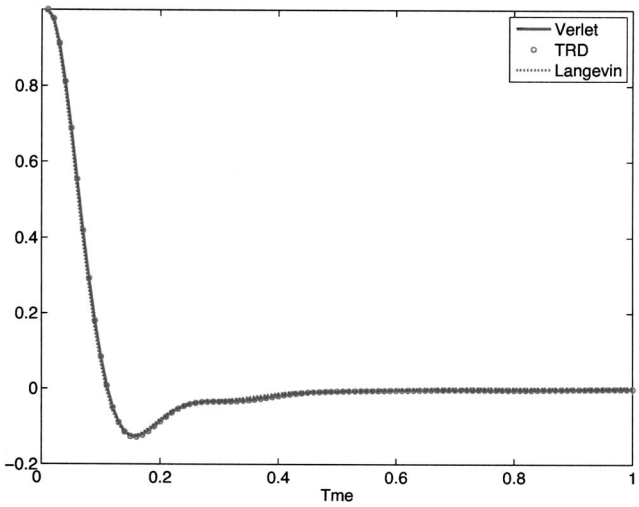

FIG. 7. Velocity autocorrelation function for solvent degrees of freedom only computed using TRD and Langevin dynamics and compared to the Verlet (*NVE*) simulation.

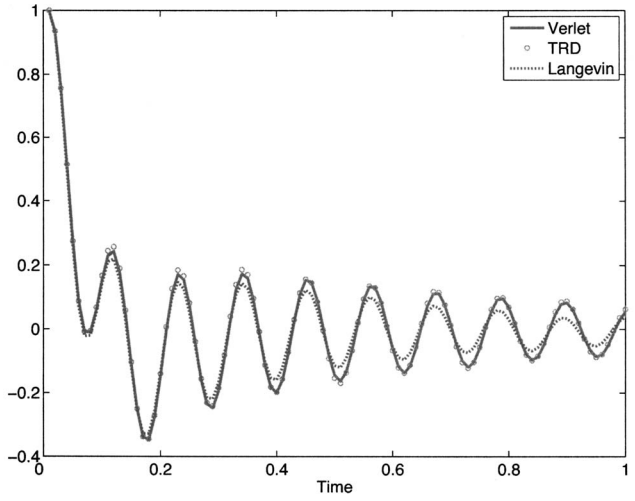

FIG. 8. Velocity autocorrelation function for vibrational degrees of freedom only computed using TRD and Langevin dynamics and compared to the Verlet (*NVE*) simulation.

with the stretch was computed using different thermostatting methods. The purpose of the model is to provide a simplified illustration of the thermal exchange process between bonded atoms and a simple molecular solvent. In all of our simulations, we used 100 000 steps of simulation using a step size of $\Delta t=0.01$, which was safely under the stability threshold.

When a thermostat is applied to a system like this, it introduces artificial perturbations to the dynamics of the model. In this experiment, we compared Langevin dynamics using the well established Brunger-Brooks-Karplus algorithm,[10] TRD, and constant energy (Verlet) simulation, all preequilibrated carefully to the desired temperature. We found that the performance of Langevin dynamics for the computation of autocorrelation functions was highly dependent on the damping coefficient γ. Obviously, a damping coefficient $\gamma=0$ would give a perfect autocorrelation function, assuming correct equilibration (since Langevin dynamics would reduce to Newtonian dynamics in that case). The choice of the time constant γ is model dependent and affects the numerical stability and strength of temperature control. In the literature of biomolecular simulation (where the 10 fs OH stretch is the shortest period), one finds a wide range of choices of the damping coefficient from a conservative 0.5/ps (Ref. 13) to a heavily damped 50/ps.[14] In our generic LJ simulations (with coefficients renormalized by the shortest period of motion), this would compare to a range of γ of 0.05–5.

Atoms in the solvent naturally relax rapidly, so their autocorrelation functions tend rapidly to zero. In Fig. 7, we superimpose the velocity autocorrelation functions computed for solvent atoms only using each of the three methods. However, looking just at the bound pair, we observed very different behaviors between, on the one hand, the dynamics-based scheme, and, on the other hand, the Langevin method, depending on the choice of Langevin damping parameter. In Fig. 8, we show the autocorrelation function for the vibrational degree of freedom, using constant energy (the target), TRD ($\mu=\tau=1$), and Langevin dynamics with $\gamma=1$. The situation is improved for smaller γ. We also tried several values of τ in TRD and found similar results in each case. Table I shows the root mean square of errors for the interval [0,2] in the calculation of the vibrational velocity autocorrelation function with various methods.

Not surprisingly, energy fluctuations for Langevin dynamics were an order of magnitude larger than for TRD, reflecting the canonical sampling. The potential for damage of the dynamics due to a too strong damping coefficient has been recognized, but large coefficients offer more powerful thermal stabilization. The typical solution is to use different values of the coefficient for various tasks; e.g., the developers of one popular code suggest the use of $\gamma=5$ ps^{-1} for the initial equilibration of molecular dynamics, followed by lower values during simulation, but point out that larger values (substantially greater than 5 ps^{-1}) may be needed if work is done on the system by the addition of (nonequilibrium) steering forces.[15] The purpose of the new TRD technique is to offer a potential adaptive solution to a wide range of thermostatting challenges, in one simulation, without the need to manually reset parameters.

VII. DISCUSSION AND CONCLUSION

The new control technique should be of interest for the general MD simulation software, i.e., as a scheme for generating temperature-regulated trajectories for various situations that involve delicate thermalization, such as for dislocation studies,[4] in the determination of nucleation rates,[5] for glassy systems (where momenta relax rapidly but configurations do so much more slowly), and for the evaluation of nonequilibrium statistical mechanics.[16] As described, the TRD scheme will be most useful for homogeneous systems that have a strong natural ergodicity property. Like Nosé–Hoover dynamics, TRD is not directly applicable to biomolecules with very different atomic masses and a network of stiff harmonic bonds.[8] For such systems, one must consider alternatives that force equilibration against the stiff restraints. One way to do this is via a more complex dynamics model. One can think of

TABLE I. Comparison of rms deviations on [0, 2] of vibrational velocity autocorrelation functions.

TRD, $\tau=0.5$	$\tau=1.0$	$\tau=0.5$	Langevin, $\gamma=0.5$	$\gamma=1.0$	$\gamma=2.0$
0.0079	0.0072	0.0082	0.0169	0.0227	0.0319

a Langevin-type approach, with different friction coefficients for the different atoms depending on their masses, or of deterministic approaches such as Nosé–Hoover chains,[17] the Hamiltonian-based recursive multiple thermostats,[18] or the generalized Gaussian moment thermostats.[19] These schemes allow a more rapid flow of energy via an active dynamical reservoir based on multiple auxiliary variables. These stronger thermostatting schemes are known to affect the resolution of time-correlation functions. We are currently investigating approaches that treat the additional variables by a TRD-like scheme, whereby the complexity of the dynamics is switched according to the thermostatting difficulty. A similar type of adaptive method based on Langevin dynamics is hinted at by our discussion of the previous section: The coupling parameter γ could be adaptively reduced as thermostatting is achieved. Finally, one could consider methods that introduce thermostatting only in specific dynamical components, such as bond stretches to hydrogen atoms, so called "targeted" thermostats. Again, this type of thermostatting could be regulated via an adaptive device along the lines of TRD.

The extension of a history-based technique like that described here in combination with different types of alternative thermostats, such as configurational thermostats[20] and dissipative particle dynamics style thermostats,[21] is under investigation by the authors.

ACKNOWLEDGMENTS

The first author acknowledges the support of the Laboratoire Jacques-Louis Lions, University of Paris VI (Pierre et Marie Curie) for a valuable visit during the preparation of this article. The third author was supported by funds from the UK Engineering and Physical Sciences Research Council. The authors thank Bruce Berne, Eric Cancès, Giovanni Ciccotti, Brian Laird, Yvon Maday, Davide Marenduzzo, Gabriel Stoltz, and Arthur Voter for comments on this work and suggestions for its application.

[1] S. Nosé, J. Chem. Phys. **81**, 511 (1984).
[2] W. Hoover, Phys. Rev. A **31**, 1695 (1985).
[3] J. Petravic and J. Delhommelle, Int. J. Thermophys. **25**, 1375 (2005).
[4] N. Weingarten and R. Selinger, J. Mech. Phys. Solids **55**(6), 1182 (2007).
[5] M. Patriarca, A. Kuronen, and K. Kaski, Current Issues in Heteroepitaxial Growth: Stress Relaxation and Self Assembly, MRS Fall Meeting Proceedings, 2001, p. 696.
[6] C. F. Sanz-Navarro, S. D. Kenny, and R. Smith, Nanotechnology **15**, 692 (2003).
[7] D. Ruelle, J. Stat. Phys. **95**, 393 (1999).
[8] E. Barth, B. Leimkuhler, and C. Sweet, *New Algorithms for Macromolecular Simulation*, Lecture Notes in Computational Science and Engineering Vol. 49 (Springer, New York, 2006), pp. 125–140.
[9] E. Cancès, F. Legoll, and G. Stoltz, Math. Modell. Numer. Anal. **41**, 351 (2007).
[10] A. T. Brunger, C. L. Brooks, and M. Karplus, Chem. Phys. Lett. **105**, 495 (1984).
[11] R. D. Skeel and J. Izaguirre, Mol. Phys. **100**, 3885 (2002).
[12] F. Legoll, M. Luskin, and R. Moeckel, Arch. Ration. Mech. Anal. **184**, 449 (2007).
[13] P. D. Blood and G. D. Voth, Proc. Natl. Acad. Sci. U.S.A. **103**, 15068 (2006).
[14] G. Widmalm and R. W. Pastor, J. Chem. Soc., Faraday Trans. **88**, 1747 (1992).
[15] T. Isgro, J. Phillips, M. Sotomayor, and E. Villa, Beckman Institute, University of Illinois, The NAMD Tutorial Report, 2007 (http://www.ks.uiuc.edu/Training/Tutorials/).
[16] H. Teramoto and S. Sasa, Phys. Rev. E **72**, 060102(R) (2005).
[17] G. Martyna, M. Klein, and M. E. Tuckerman, J. Chem. Phys. **97**, 2635 (1992).
[18] B. Leimkuhler and C. Sweet, SIAM J. Appl. Dyn. Syst. **4**, 187 (2005).
[19] Y. Liu and M. E. Tuckerman, J. Chem. Phys. **112**, 1685 (2000).
[20] C. Braga and K. P. Travis, J. Chem. Phys. **123**, 134101 (2005).
[21] M. P. Allen and F. Schmid, Mol. Simul. **33**, 21 (2007).